4.0 Summary

In this chapter, a comparative study between different permalloy materials were reported by varying the annealing temperature, cooling rate and holding time in the presence of hydrogen atmosphere. The effect of alloy composition on the structural and magnetic properties of Ni-Fe alloys has been explained. The results have been discussed in terms of correlation between microstructures, X-ray diffractographs and their magnetic properties.

4.1 Introduction

The magnetic properties of the permalloys not only depend on the heat treatment under hydrogen atmosphere but also depend on the degree of short-range order (SRO) developed in the materials [1]. Optimum magnetic properties were obtained when a critical degree of SRO is developed in these alloys, which allow both the anisotropy energy and magnetostriction constant to be simultaneously reduced to small values. Various degrees of order can be obtained by controlled cooling of the specimens at different rates in the temperature range between about 500°C and 400°C. The structure sensitive magnetic properties such as coercivity, permeability and core loss of the Ni-Fe alloys also depend on the microstructure [2-15]. Here a comparative study between three different permalloy samples was carried out (more detail are given in chapter 3).

4.2 Structural analysis

Fig. 4.1 shows the variation of the lattice parameter of the three samples, sample A, sample B and sample C as a function of annealing temperature [16-17]. From the figure, it can be seen that at 1150°C, the lattice parameter is greater for sample C (3.58 A^o) as compared to sample A (3.54 A^o). It shows that the lattice parameter of Ni-Fe alloys is composition dependent [18]. Also, the lines in the figure shows that sample C orders slightly more rapidly than the sample A and therefore possibly the SRO developed in the sample A gives rise to highest permeability in the material in comparison to the other materials [1, 19].

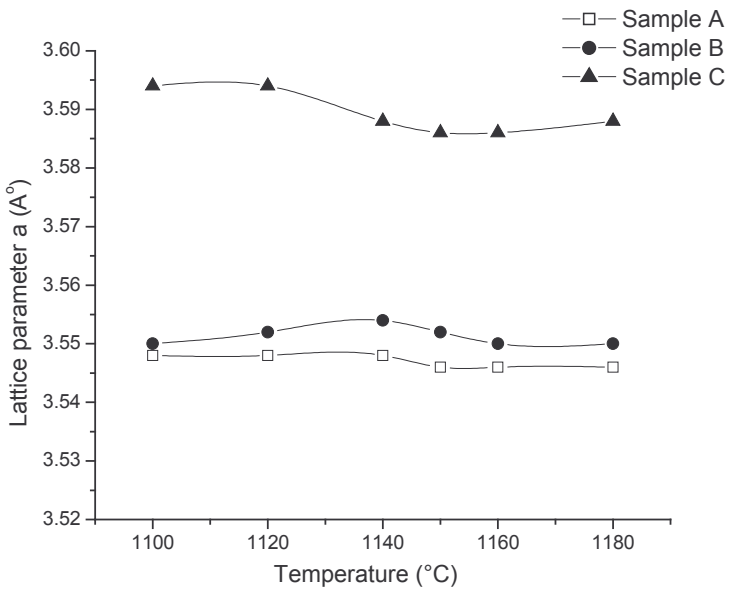

Fig. 4.1: Lattice parameter 'a' of sample A, sample B and sample C as a function of annealing temperature

Fig. 4.2 shows the optical microstructures of the samples A, B and C at 100 X magnification. The grain structure reflects the variation in grain diameter on increase in the Ni content. The twin structure appears at the grain boundaries as seen. A comparative grain structure reveals that relatively larger grain diameter (320 μm) obtained in sample A as compared to sample B (277 μm) and sample C (127 μm) result in the enhanced permeability and other magnetic effects.

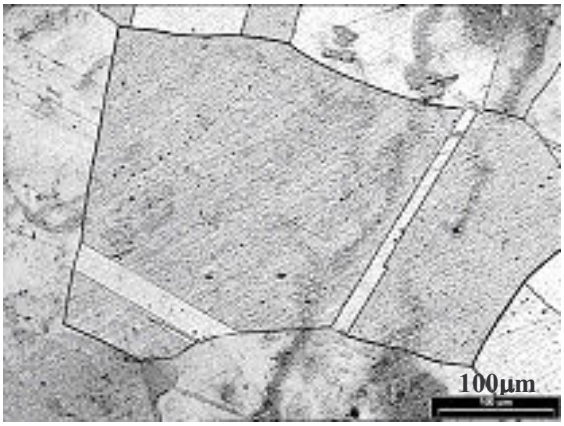

a)

Average grain diameter = 320 µm

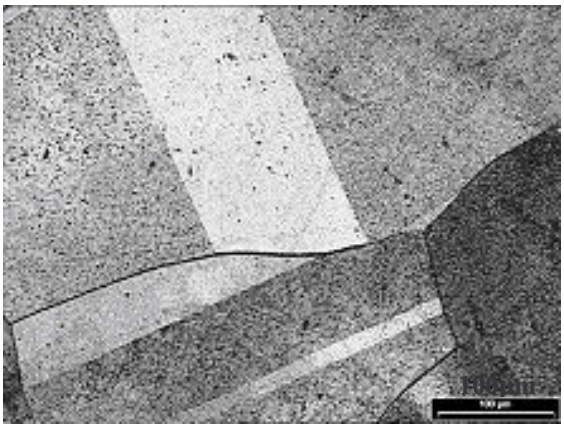

b)

Average grain diameter = 277 µm

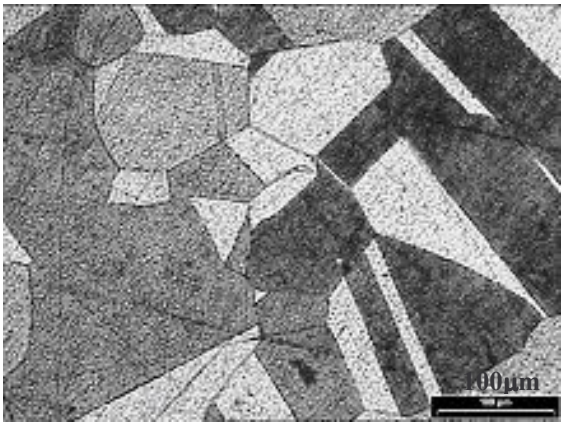

c)

Average grain diameter = 127 µm

Fig. 4.2: Optical micrographs of a) sample A, b) sample B and c) sample C at 100X magnification

4.3 Magnetic measurements

The AC magnetic properties of the three samples were compared to understand the effect of alloy composition on the properties.

The remanence of sample A, sample B and sample C shows variations as a function of annealing temperature, cooling rate and holding time as shown in Table 4.1 (a-c) and in Fig. 4.3 (a-c) respectively. At 300 Hz and at a temperature of 1100°C, the remanence in sample A is 499 mT and in sample B is 545 mT and highest for sample C, 1173 mT as shown in Fig. 4.3a. Similar values were observed at other higher temperatures. Similarly, at cooling rate of 2°C/min., the remanence in sample A is 511 mT, in sample B is 569 mT and in sample C is 1169 mT as shown in Fig. 4.3b. These observations were taken at a temperature of 1150°C and holding time of 2 h. Similarly, for holding time of 2 h, the remanence in sample A is 465 mT, in sample B is 575 mT and in sample C is 1182 mT as shown in Fig. 4.3c. We concluded that the remanence as a function of various process parameters is highest in sample C and is least in sample A.

The coercivity of sample A, sample B and sample C also shows variations as a function of annealing temperature, cooling rate and holding time as can be seen in Table 4.2 (a-c) and in Fig. 4.4 (a-c) respectively. At 300 Hz and at a temperature of 1100°C, the coercivity in sample A is 25 A/m and in sample B, is 78 A/m and highest for sample C, 255 A/m as shown in Fig. 4.4a. Similar behaviour has been seen at other higher temperatures. Similarly, at cooling rate of 2°C/min., the coercivity in sample A is 25 A/m, in sample B is 82 A/m and in sample C is 254 A/m as shown in Fig. 4.4b. These observations were taken at a temperature of 1150°C and holding time of 2 h. Also, for a holding time of 2 h, the coercivity in sample A is 24 A/m, in sample B is 82 A/m and in sample C is 256 A/m as shown in the Fig. 4.4c. We concluded that the coercivity as a function of various process parameters is least in sample A and highest in sample C, due to the reason that coercivity is inversely proportional to the grain diameter [15, 20] and the grain diameter of sample A is larger (320 μm) as compared to sample B (277 μm) and sample C (127 μm).

Table 4.1a: Effect of annealing temperature on remanence (B_r)

Annealing temperature (°C)	Sample A (mT)	Sample B (mT)	Sample C (mT)
1100	499.82	545.26	1173.10
1120	505.08	549.23	1088.86
1140	501.26	577.58	1175.28
1150	465.35	575.71	1182.63
1160	491.89	572.42	1177.19
1180	508.74	555.26	1107.15

Table 4.1b: Effect of cooling rate on remanence (B_r)

Cooling rate (°C/min.)	Sample A (mT)	Sample B (mT)	Sample C (mT)
2.0	511.93	569.32	1169.12
2.5	465.35	575.71	1182.63
3.0	475.33	572.76	1130.77
5.0	494.20	590.40	1170.58
7.0	470.28	602.53	1105.35

Table 4.1c: Effect of holding time on remanence (B_r)

Holding time (h)	Sample A (mT)	Sample B (mT)	Sample C (mT)
1	482.89	580.49	1164.56
2	465.35	575.71	1182.63
3	474.99	575.66	1197.19

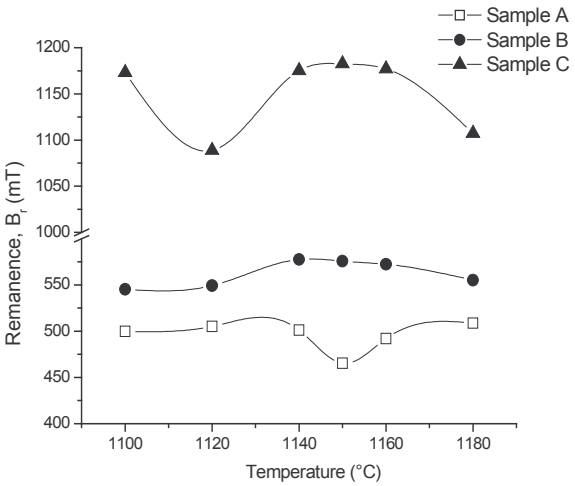

(a)

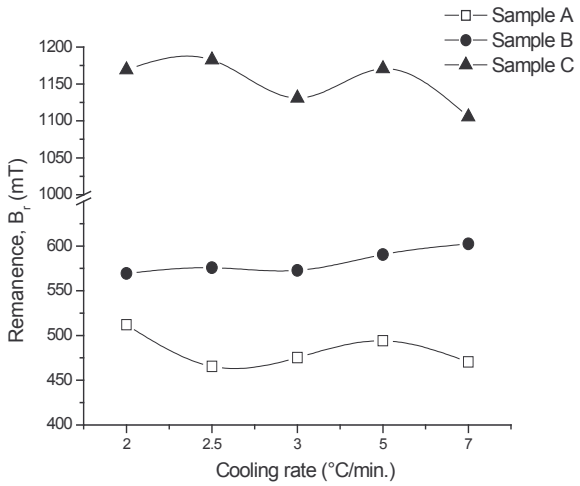

(b)

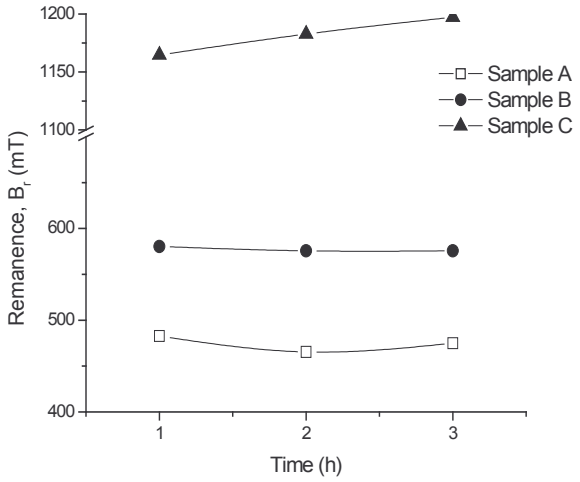

(c)

Fig. 4.3: Effect of alloy composition on remanence

Table 4.2a: Effect of annealing temperature on coercivity (H_c)

Annealing temperature (°C)	Sample A (A/m)	Sample B (A/m)	Sample C (A/m)
1100	25.06	78.51	255.78
1120	25.30	82.47	245.69
1140	25.05	83.74	251.96
1150	24.49	82.70	256.25
1160	24.51	82.23	254.41
1180	25.23	85.01	249.38

Table 4.2b: Effect of cooling rate on coercivity (H_c)

Cooling rate (°C/min.)	Sample A (A/m)	Sample B (A/m)	Sample C (A/m)
2.0	25.30	82.34	254.20
2.5	24.49	82.70	256.25
3.0	24.65	87.46	253.59
5.0	24.78	85.11	255.63
7.0	24.43	87.66	248.23

Table 4.2c: Effect of holding time on coercivity (H_c)

Holding time (h)	Sample A (A/m)	Sample B (A/m)	Sample C (A/m)
1	23.05	84.71	262.52
2	24.49	82.70	256.25
3	24.68	83.95	254.30

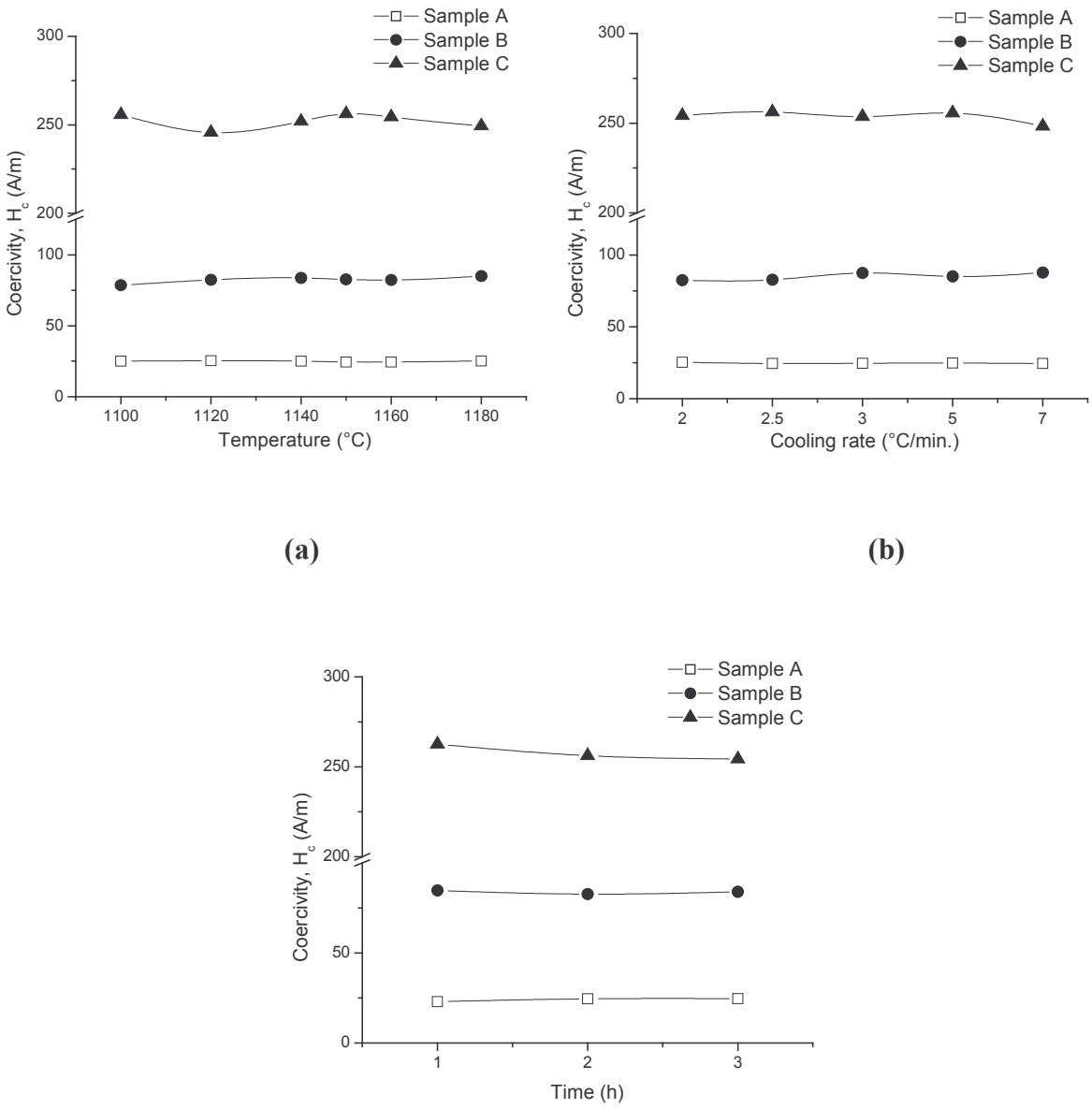

Fig. 4.4: Effect of alloy composition on coercivity

The peak permeability of sample A, sample B and sample C as a function of annealing temperature, cooling rate and holding time is given in Table 4.3 (a-c) and in Fig. 4.5 (a-c) respectively. At 300 Hz and at a temperature of 1100°C, the peak permeability in sample A is 10309 and in sample B is 3000 and in sample C is 2370 as shown in Fig. 4.5a. Similar values were observed at other higher temperatures. Similarly, at cooling rate of 2°C/min., the peak permeability in sample A is 10478, in sample B is 2981 and in sample C is 2387 as shown in Fig. 4.5b. These observations were taken at a temperature of 1150°C and holding time of 2 h. Also, for a holding time of 2 h, the peak permeability of sample A is 9954, in sample B is 2950 and in sample C is 2364 as shown in Fig. 4.5c. From the above results, we concluded that the permeability of the sample A is highest and sample C is least which is due to the reason that permeability is directly proportional to the grain diameter and the grain diameter in sample A is high (320 μm) therefore, the domain wall motion is easy in sample A which gives rise to the highest permeability of sample A. Also, the presence of Mo element in sample A and sample B, slow down the ordering kinetics and lowers the degree of long range order thereby increase the resistivity and simplifies the final heat treatment and hence improves the properties such as permeability and other magnetic properties. Actually, the addition of non-ferromagnetic elements such as Mo decreases the proportion of magnetic nickel atoms, thereby reducing the density of the magnetic atom interactions, which are responsible for the magnetostriction and the anisotropy [19-22].

The core loss of sample A, sample B and sample C as a function of annealing temperature, cooling rate and holding time is given in Table 4.4 (a-c) and in Fig. 4.6 (a-c) respectively. At 300 Hz and at a temperature of 1100°C, the core loss in sample A is 5 mW and in sample B is 10 mW and highest for sample C is 59 mW as shown in Fig. 4.6a. Similarly, at cooling rate of 2°C/min., the core loss in sample A is 5 mW, in sample B is 11 mW and in sample C is 59 mW as shown in Fig. 4.6b. These observations were taken at a temperature of 1150°C and holding time of 2 h. Also, for a holding time of 2 h, the core loss in sample A is 9 mW, in sample B is 11mW and in sample C is 59 mW as shown in Fig. 4.6c. As the theory explains that the losses are inversely proportional to the grain diameter, therefore the core loss is minimum in sample A, due to the bigger grain

diameter in sample A (320 μm) and maximum in sample C due to smaller grain diameter (127 μm).

Table 4.3a: Effect of annealing temperature on peak permeability

Annealing temperature (°C)	Sample A	Sample B	Sample C
1100	10309	3000	2370
1120	10206	2947	2394
1140	10648	2996	2376
1150	9954	2950	2364
1160	10460	2972	2390
1180	10330	2930	2395

Table 4.3b: Effect of cooling rate on peak permeability

Cooling rate (°C/min.)	Sample A	Sample B	Sample C
2.0	10478	2981	2387
2.5	9954	2950	2364
3.0	10018	3027	2394
5.0	10583	2981	2368
7.0	10080	3014	2400

Table 4.3c: Effect of holding time on peak permeability

Holding time (h)	Sample A	Sample B	Sample C
1	10026	2948	2344
2	9954	2950	2364
3	10122	2971	2386

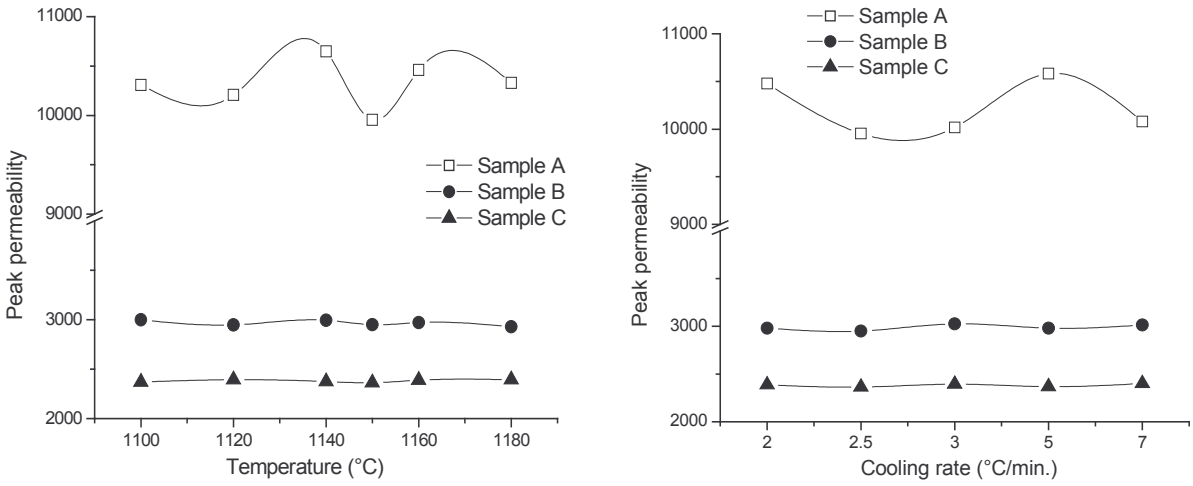

(a) **(b)**

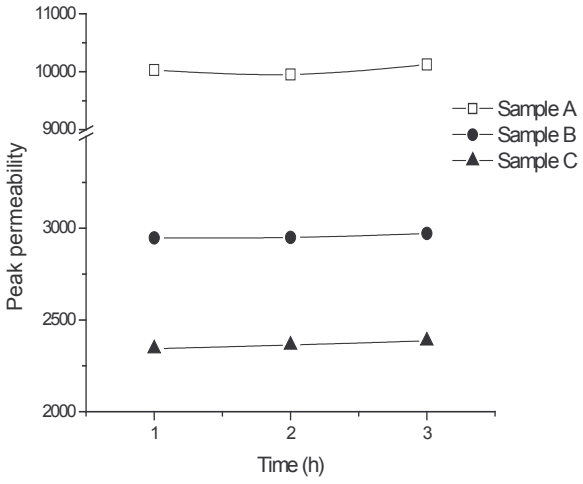

(c)

Fig. 4.5: Effect of alloy composition on peak permeability

Table 4.4a: Effect of annealing temperature on core loss (P_c)

Annealing temperature (°C)	Sample A (mW)	Sample B (mW)	Sample C (mW)
1100	5	10	59
1120	5	11	56
1140	5	11	59
1150	5	11	59
1160	5	11	59
1180	5	11	58

Table 4.4b: Effect of cooling rate on core loss (P_c)

Cooling rate (°C/min.)	Sample A (mW)	Sample B (mW)	Sample C (mW)
2.0	5.5	11	59
2.5	5.0	11	59
3.0	5.1	12	58
5.0	5.4	11	59
7.0	5.1	12	57

Table 4.4c: Effect of holding time on core loss (P_c)

Holding time (h)	Sample A (mW)	Sample B (mW)	Sample C (mW)
1	9	11	60
2	9	11	59
3	5	11	59

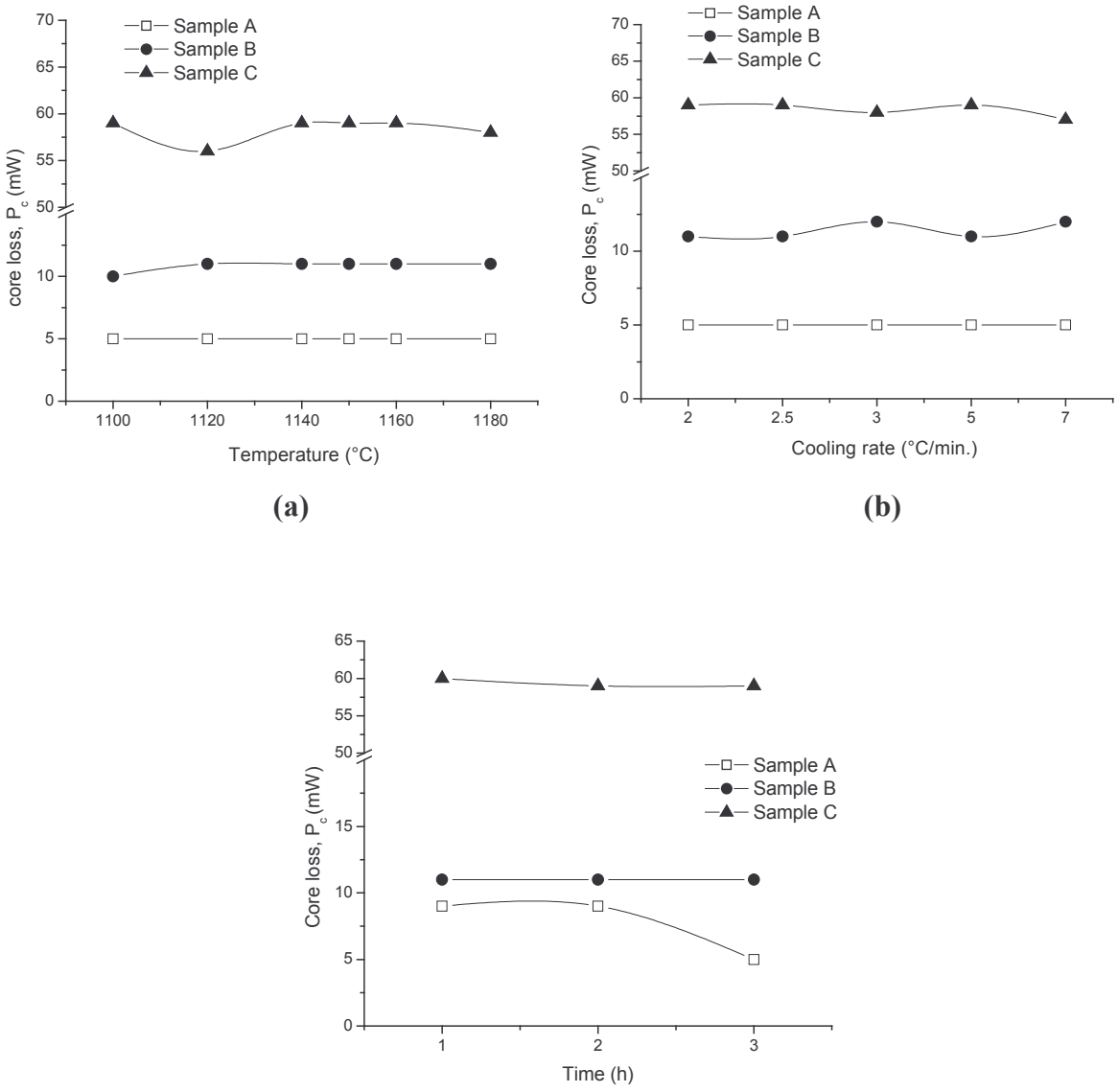

Fig. 4.6: Effect of alloy composition on core loss

References

1. T. Akomolafe & G. W. Johnson, J. Mater. Sci., **24** (1989) 349
2. D. W. Dietrich, ASM handbook: Magnetically soft materials, properties and selection : non-ferrous alloys and special purpose materials, ASM International, **2** (1990) 761
3. F. Pfeifer & C. Radeloff, J. Magn. Magn. Mater., **19** (1980) 190
4. M. A. Da Cunha & S. C. Paolinelli, Mater. Res., **5** (2002) 373
5. C. M. B. Bacaltchuk, Effect of magnetic annealing on texture and microstructure development in silicon steel, Ph.D thesis (2005)
6. S. P. Narayan, V. Rao, S. Das & O. N. Mohanty, J. Magn. Magn. Mater., **88** (1990) 71
7. D. Bahadur, W. Fischer & M. V. Rane, Mater. Sci. & Engg., **252** (1999) 109
8. H. H. Scholefield, R.V. Major, B. Gibson & A. P. Martin, Brit. J. Appl. Phys., **18** (1967) 41
9. R. D. Enoch & A. D. Fudge, Brit. J. Appl. Phys., **17** (1966) 623
10. R. M. Bozorth, Ferromagnetism (D van Nostrand Company Inc., New York, London, Toronto), 1951
11. V. Shemet, M. Yurechko, A. K.Tyagi, W. J. Quadakkers & L. Singheiser, Miner. Met. Mater. Soc., USA (1999) 783
12. Kiran Gupta, K. K. Raina & S. K. Sinha, Ind. J. Engg. Mater. Sci., **12** (2005) 577
13. Kiran Gupta, K. K. Raina & S. K. Sinha, Bull. Mater. Sci., **29** (2006) 391
14. Kiran Gupta, S. K. Sinha & K. K. Raina, Proc. Nat. conf. on materials for electrical, electronic & magnetic applications: characterisation & measurements, Hyderabad, DMRL (2005) 6B.5
15. F. Pfeifer, Encyclo. Mater. Sci. Engg., **4** (1986) 2663
16. JCPDS-International Centre for Diffraction Data, PCPDFWIN, **2.02** (1999)
17. B. D. Cullity, Elements of X-ray diffraction, 3rd ed., Prentice –Hall, Upper Saddle River, N J, 2001
18. R. C. Jackson & E.W. Lee, J. Mater. Sci., **1** (1966) 362
19. T. Akomolafe & G. W. Johnson, J. Mater. Sci., **23** (1988) 790

20. G. Herzer, IEEE Trans. Magn., **26** (1990) 1397
21. E. G. Taylor & G. W. Johnson, J. Mater. Sci., **12** (1977) 51
22. S. Preston & G. W. Johnson, J. Mater. Sci., **19** (1984) 4099